MESOANTICYCLONES AND ANTICYCLONIC TORNADOES IN SUPERCELLS

Howard B. Bluestein, Jeffrey C. Snyder, and Michael M. French

School of Meteorology, University of Oklahoma, 120 David L. Boren Blvd., Suite 5900, Norman, OK 73072,U. S. A., hblue@ou.edu

(Dated: 26 August 2011)

I. INTRODUCTION

Anticyclonic tornadoes and mesoanticyclones have been documented or inferred in right-moving supercells (e.g., Fujita 1963; Lemon 1976; Brown and Knupp 1980; Fujita 1981; Bluestein and Gaddy 2001; Bluestein et al. 2007; Bluestein et al. 2010; Tanamachi et al. 2012) (Figs. 1, 2), but they are found less frequently than cyclonic tornadoes and mesocyclones. Anticyclonic vortices are seen in left-moving supercells, but anticyclonic tornadoes in them are extremely rare (e.g., Bunkers and Stoppkotte 2007). The purpose of this paper is to show evidence from a decade of storm-intercept activities, including mobile Doppler-radar documentation, of anticyclonic tornadoes and meso-anticyclones in right-moving supercells, to generalize our findings, and to hypothesize why these features occur.

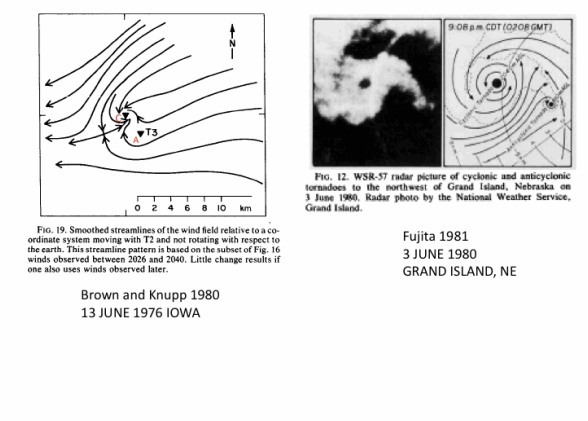

FIG. 1: Inferred streamlines and locations of cyclonic-anticyclonic tornado pairs in supercells; radar reflectivity also shown (right).

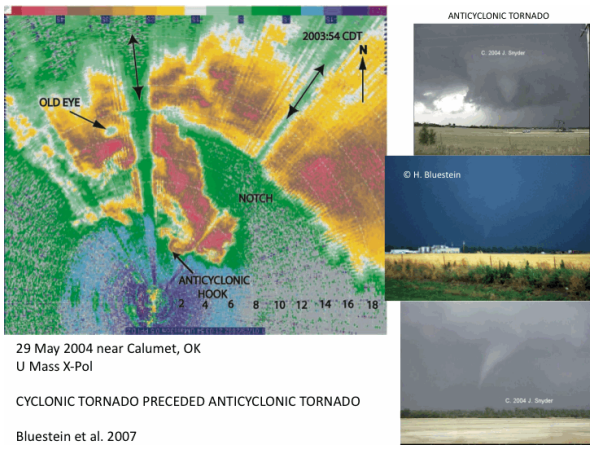

FIG. 2: Photographs (right) of an anticyclonic tornado and mobile Doppler-radar reflectivity PPI from the UMass XPol (left). "Up" points to the north. The anticyclonic tornado formed after the cyclonic tornado had dissipated (Bluestein et al. 2007).

II. DOPPLER-RADAR OBSERVATIONS

A non-exhaustive, but representative, selection of radar imagery and photographs of anticyclonic tornadoes and meso-anticyclones is shown in Figs. 2 – 15.

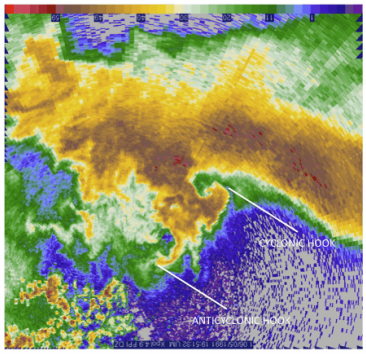

FIG. 3: Cyclonic and anticylonic hook echoes in a supercell, from the mobile U. Mass. X-band radar.

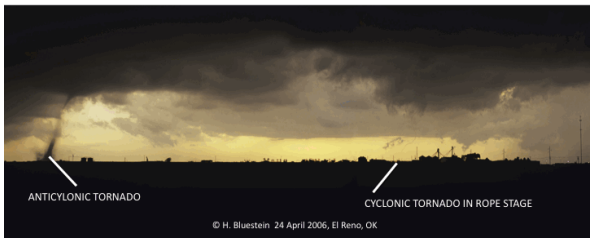

FIG. 4: Photographs of a cyclonic-anticyclonic tornado pair. The anticyclonic tornado formed as the cyclonic tornado was dissipating.

III. SUMMARY AND CONCLUSIONS

In right-moving supercells there are two basic types of mesoanticyclones. (1) anticyclonic midlevel vortex that is part of the cyclonic-anticyclonic vortex couplet produced by the tilting of environmental horizontal vorticity associated with vertical wind shear at the edge of the main updraft, sometimes on the left flank, to the left of the WER; (2) anticyclonic member of cyclonic-anticyclonic couplet along the rear-flank gust front associated with anticyclonic shear at southern end of the RFD, possibly due to the tilting

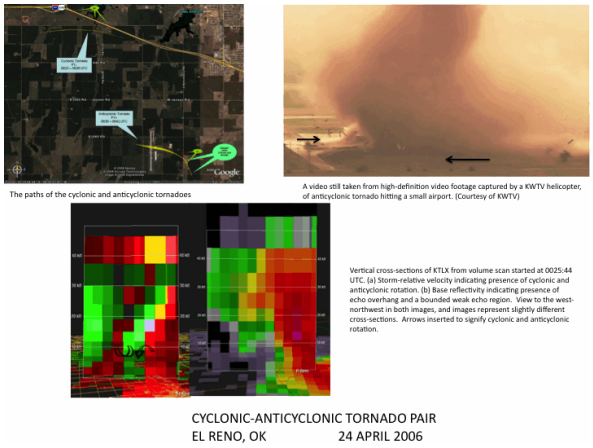

FIG. 5: Tracks of the cyclonic-anticyclonic tornado pair seen in Fig. 4 (upper left), frame from television helicopter video of the anticyclonic tornado (upper right), and KTLX Doppler velocities and reflectivity as a function of height (lower). (courtesy of Jeff Snyder)

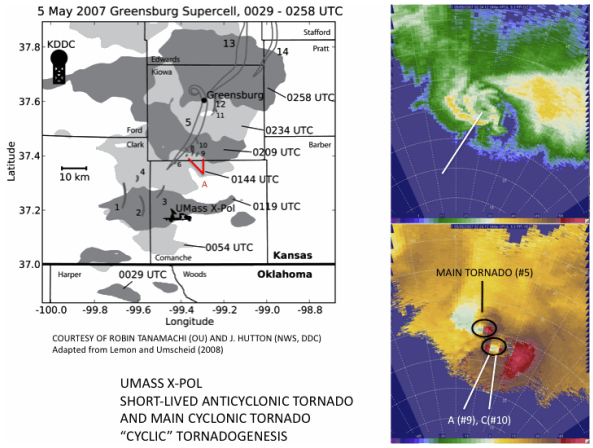

FIG. 6: Damage paths of tornadoes and KDDC depictions of radar echo at selected times for the Greensburg, KS tornado family (left) and UMass X-Pol reflectivity (upper right) and Doppler velocity (lower right) for a cyclonic-anticyclonic tornado pair (Tanamachi et al. 2012, in review).

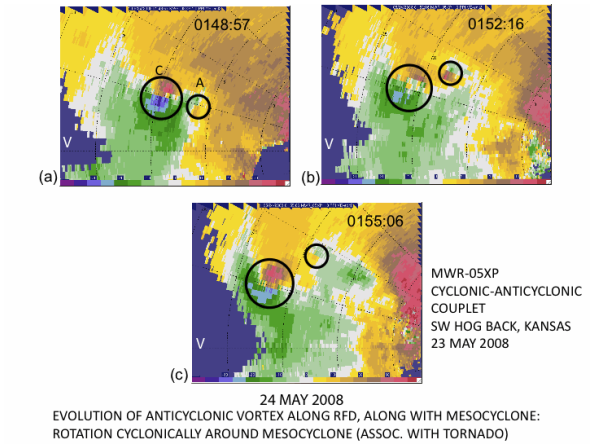

FIG.7: Doppler velocity field exhibiting cyclonic-anticyclonic couplet, with anticyclonic member rotating cyclonically about the cyclonic member, from rapid-scan, MWR-05XP data (Bluestein et al. 2010).

of baroclinically generated horizontal vorticity at the line

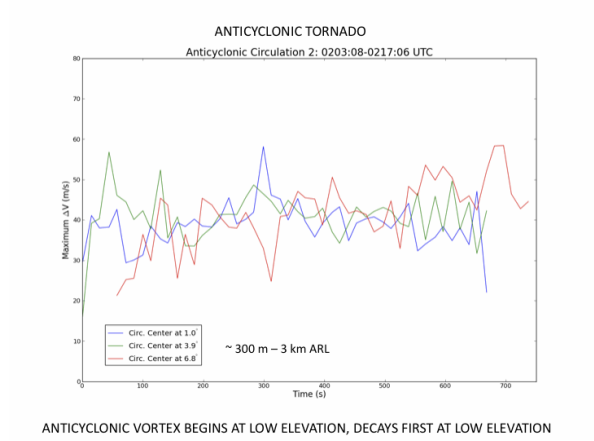

FIG. 8: Evolution of anticyclonic Doppler-velocity shear for an anticyclonic tornado on 23 May 2008, as a function of time at three levels, from MWR-05XP rapid-scan data. The vortex first appears at low-elevation angle and builds upward, and first dissipates at low elevation angle and later aloft. (from M. French's Ph. D. thesis, in progress)

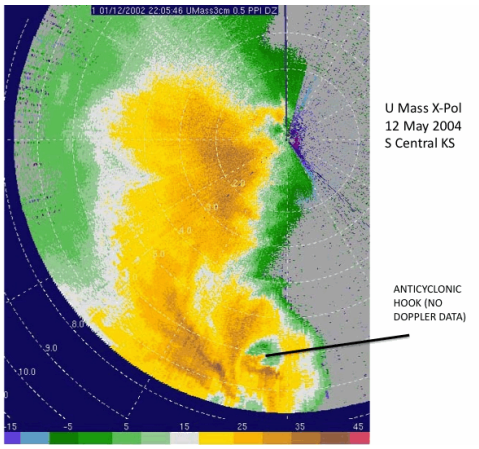

FIG. 9: Anticyclonic hook associated with a supercell that produced cyclonic tornadoes. In this case only up points to the east.

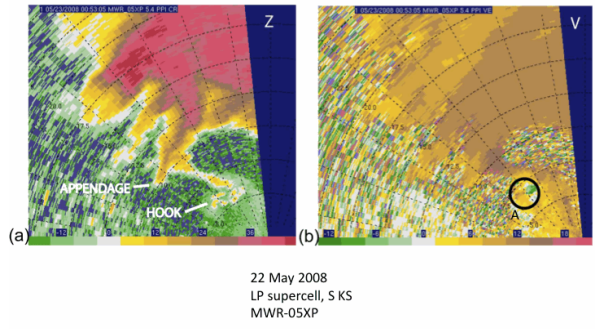

FIG. 10: Reflectivity field showing an anticyclonic hook (left) with anticyclonic shear (right) from MWR-05XP rapid-scan data.

end (e.g., Markowski et al. 2008). Some may be related to the "Owl Horn echo" (Kramar et al. 2005). Anticyclonic tornadoes, in a few instances for which we have good documentation, begin near the surface and build upwards with time, form after nearby cyclonic tornadoes do, and are *not* the mirror images of tornadoes in left-moving supercells.

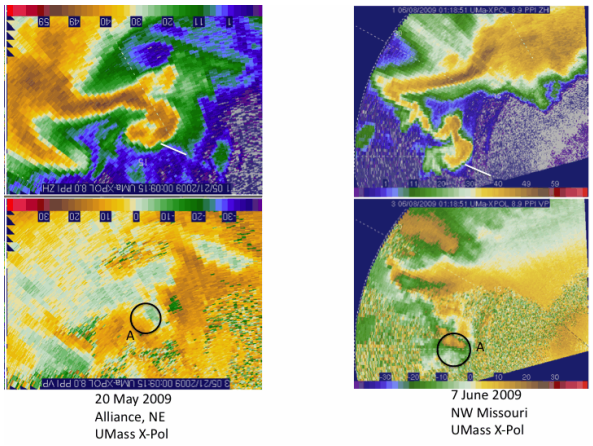

FIG. 11: Anticyclonic hooks in reflectivity (top) and anticyclonic Doppler shear (bottom) from the UMass X-Pol during VORTEX2.

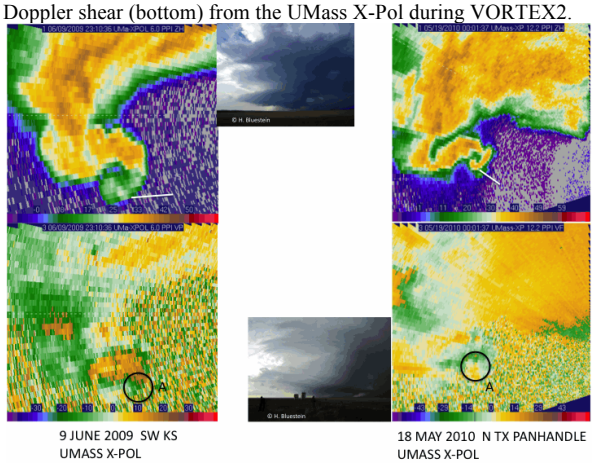

FIG. 12: As in Fig. 11, but photographs also shown.

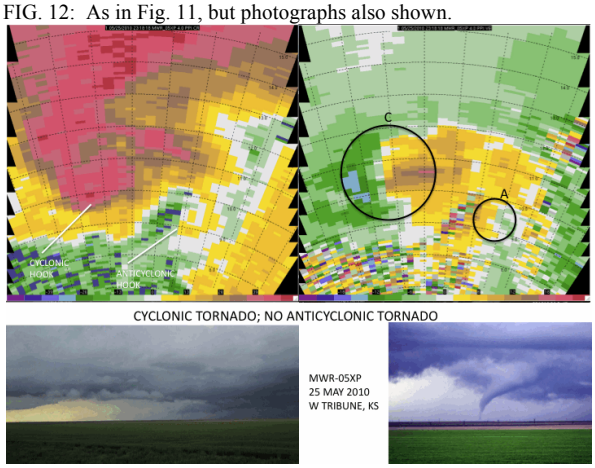

FIG. 13: As in Fig. 11, but only for one case; photographs shown below for wide view (left) and close-in view on cyclonic tornado.

IV. ACKNOWLEDGMENTS

This research was supported by NSF grant AGS-0934307 and earlier grants. Stephen Frasier and graduate students (UMass, OU) participated in the collection and processing of data with the U. Mass. X-band/X-Pol mobile Doppler radar; Robert Bluth (NPS), Ivan PopStefanija and colleagues did the same for the MWR-05XP.

V. REFERENCES

Bluestein, H. B., and S. G. Gaddy, 2001: Airborne pseudo-dual-Doppler analysis of a rear-inflow jet and deep convergence zone within a supercell. *Mon. Wea. Rev.*, **129**, 2270 – 2289.

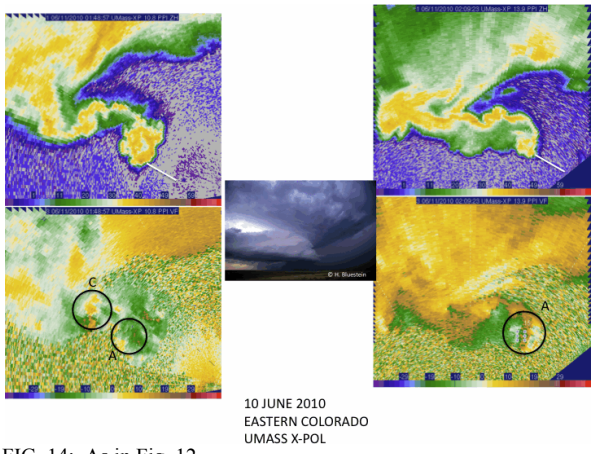

FIG. 14: As in Fig. 12.

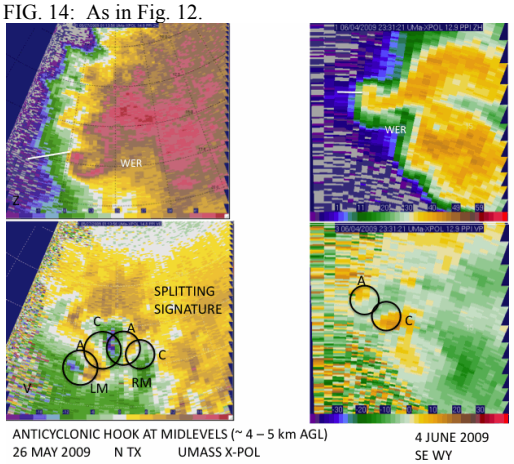

FIG. 15: As in Fig. 11, but at midlevels.

Bluestein, H. B., M. M. French, R. L. Tanamachi, S. Frasier, K. Hardwick, F. Junyent, and A. L. Pazmany, 2007: Close-range observations of tornadoes in supercells made with dual-polarization, X-band, mobile Doppler radar. *Mon. Wea. Rev.*, **135**, 1522 – 1543.

Bluestein, H. B., M. M. French, I. PopStefanija, R. T. Bluth, and J. B. Knorr, 2010: A mobile, phased-array Doppler radar for the study of severe convective storms. *Bull. Amer. Meteor. Soc.*, **91**, 579 – 600.

Brown, J. M., and K. R. Knupp, 1980: The Iowa cyclonic-anticyclonic tornado pair and its parent thunderstorm. *Mon. Wea. Rev.*, **108**, 1626 – 1646.

Bunkers, M. J., and J. W. Stoppkotte, 2007: Documentation of a rare tornadic left-moving supercell. *Electr. J. Sev. Storms Meteor.*, **2**(2), 1–22.

Fujita, 1963: Analytical mesometeorology: A review. *Severe Local Storms. Meteor. Monogr.*, **5**, no. 27, Amer. Meteor. Soc., 77 – 125.

Fujita, T. T., 1981: Tornadoes and downbursts in the context of generalized planetary scales. *J. Atmos. Sci.,* **38**, 1511 – 1534.

Kramar, M. R., H. B. Bluestein, A. L. Pazmany, and J. D. Tuttle, 2005: The "Owl Horn" radar signature in developing Southern Plains supercells. *Mon. Wea. Rev.*, **133**, 2608 – 2634.

Lemon, L., 1976: Wake vortex structure and aerodynamic origin in severe thunderstorms. *J. Atmos. Sci.*, **33**, 678 – 685.

Markowski, P., E. Rasmussen, J. Straka, R. Davies-Jones, Y. Richardson, and R. J. Trapp, 2008: Vortex lines within low-level mesocyclones obtained from pseudo-dual-Doppler radar observations. *Mon. Wea. Rev.*, **136**, 3513 – 3535.

Tanamachi, R. L., H. B. Bluestein, J. B. Houser, S. J. Frasier, and K. M. Hardwick, 2012: Mobile, X-band, polarimetric Doppler radar observations of the 4 May 2007 Greensburg, Kansas tornadic supercell. *Mon. Wea. Rev.* (in review)